Voltage-Driven Molecular Catalysis: a Promising Approach to Electrosynthesis

Koushik Barman,[†] Yu Chen,[†,§] Shu Wu,[†,§] Guoxiang Hu,[†,§,%,*] and Michael V. Mirkin[†,#,*]

† Department of Chemistry and Biochemistry, Queens College-CUNY, Flushing, NY 11367, US
§ The Graduate Center of CUNY, New York, NY 10016.
# Advanced Science Research Center at The Graduate Center, CUNY; New York, NY 10031.
% Present address: School of Materials Science and Engineering, Georgia Institute of Technology, Atlanta, GA 30332, US

Corresponding Author
E-mail: emma.hu@mse.gatech.edu, *mmirkin@qc.cuny.edu*

ABSTRACT

The combination of electrocatalysis and molecular catalysis is an increasingly popular approach to designing catalysts for electrosynthetic processes. We found recently that the electrostatic potential drop across the double layer contributes to the driving force for electron transfer between a dissolved reactant and a molecular catalyst immobilized directly on the electrode surface. The applied electrode potential can increase the oxidizing (or reducing) ability of a surface-bound molecular catalyst, thus, making it suitable for charge-transfer processes, which it normally would not be able to catalyze. In this Article, we report the initial application of voltage-driven molecular catalysis to electroorganic synthesis. The metal-free, purely organic molecular catalyst (TEMPO) attached to a carbon electrode showed potential-dependent activity for the oxidation of toluene, which does not occur if TEMPO is used as a homogeneous catalyst. Surface-attached TEMPO also shows significant catalytic activity towards benzyl alcohol oxidation even at pH 7. The products of toluene and benzyl alcohol oxidations were identified by NMR, FTIR, and UV-VIS spectroscopies to evaluate the reaction yield and selectivity. The effect of the applied electrode potential on these catalytic processes was elucidated by DFT calculations.

Keywords: voltage-driven molecular catalysis, electrocatalysis, TEMPO, electroorganic synthesis, oxidation of toluene and benzyl alcohol

INTRODUCTION

Most of the reported applications of electrocatalysis in synthetic chemistry make use of molecular mediators serving as homogeneous redox catalysts.[1-6] Such mediators facilitate oxidation/reduction processes, offer improved selectivity, and eliminate problems caused by passivation and contamination of heterogeneous catalyst surfaces.[2,4] However, the applied electrode potential cannot be used as a means to drive homogeneous catalytic reactions, which, therefore, require potent oxidizing and reducing chemical agents.

Unlike molecular catalysis, heterogeneous electrocatalytic processes occur on active surface sites and are driven by the applied electrode potential.[7,8] Recent studies focused on the advantages of combining molecular catalysts and electrocatalysts into hybrid systems for energy-related processes.[7,9-12] Hybrid molecular catalysts possess key advantages of homogeneous catalysts and heterogeneous electrocatalysts: they are typically noble-metal-free, do not suffer from passivation, and do not require complex engineering and characterization of active sites essential for heterogeneous electrocatalysts. Unlike a homogeneous catalyst, which is often irrecoverable or requires significant energy for its separation from reaction products,[13,14] the amount of the surface-bound redox mediator is typically small, no separation is required, and the catalyst modified surface can be re-used for electrosynthesis.

Direct coupling of catalysts to carbon electrodes reported by the Surendranath group produced tunable heterogeneous catalysts with molecularly well-defined active sites.[15-17] The molecules conjugated to carbon became part of the electrode, so that no electron transfer (ET) occurred between the electrode and a catalytic moiety whose oxidation state remained unchanged.[17] By contrast, in voltage-driven catalysis the potential drop across the electrical double layer (EDL) is distributed on both sides of the attached molecular catalyst immobilized directly on

the electrode surface.[18] A fraction of the applied potential dropping between the electrode and the attached molecular catalyst causes its oxidation/reduction, while the other fraction of the applied potential dropping between the surface-bound catalyst and the dissolved reactant drives the electrocatalytic process (Fig. 1).

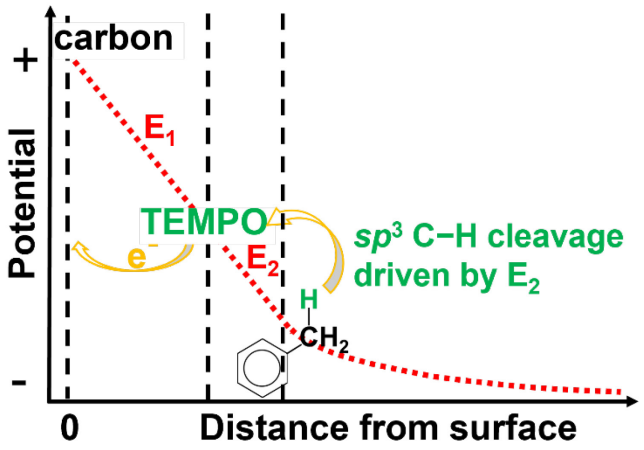

Fig. 1. Voltage-driven catalysis of toluene oxidation by TEMPO molecules directly attached to the carbon surface. Scheme of the potential drop (red dotted line) across the carbon electrode/solution interface. A fraction of the applied potential drops between the surface-attached TEMPO and a dissolved toluene molecule.

The contribution of the electrode potential to the driving force for ET between an immobilized molecular catalyst and a dissolved reactant in voltage-driven catalysis enabled the use of a molecular catalyst with a standard potential lower than that normally required for water oxidation and other processes.[19] In this Article, we report the first application of voltage-driven molecular catalysis to electrosynthesis – the oxidations of alcohols and toluene in aqueous/organic solvents by TEMPO (2,2,6,6-tetramethyl-1-piperidine N-oxyl; a fully organic molecular catalyst extensively employed for electrosynthesis[20,21]) immobilized on a carbon electrode surface. A schematic representation of the TEMPO-modified electrode is shown in Fig. S1. Cyclic aminoxyl species have previously been employed to catalyze the oxidation of alcohols to the corresponding

aldehydes, ketones, and carboxylic acids.[22-25] Specifically, TEMPO radical has been extensively used as a homogeneous alcohol oxidation catalyst in aqueous solutions.[26-29] One problem in such applications is the low solubility of TEMPO in polar electrolytic media.[30] It was circumvented by attaching TEMPO to the electrode surface, e.g., by covalently immobilizing it onto linear poly-(ethylenimine) and cross-linking onto the surface of a glassy carbon electrode [31] or by noncovalent immobilization of a pyrene-TEMPO conjugate.[32] A TEMPO-modified electrode exhibited higher current density than the TEMPO-based homogeneous catalytic system.[31]

TEMPO exhibits modest activity for oxidation of benzyl alcohol (BzOH) in a neutral aqueous solution either as a homogeneous catalyst[33] or when immobilized on polymer coated surfaces.[34,35] A comparative study of BzOH oxidation with several nitroxyl derivatives showed that the catalytic activity is largely affected by the driving force, i.e., the catalyst standard potential.[29] Here we show that in voltage-driven catalysis with surface-bound TEMPO the driving force is augmented by the applied anodic bias, resulting in a significant catalytic activity towards BzOH oxidation to benzaldehyde even at pH 7. The mechanism of TEMPO-catalyzed electrooxidation of BzOH in organic solvents involves base-promoted formation of the $TEMPO^{+}$/alkoxide adduct, followed by turnover-limiting intramolecular hydrogen transfer within this complex.[36] Our density functional theory (DFT) calculations show that the applied voltage can decrease the activation energy for this step, thereby increasing the reaction rate. Besides, we show that further oxidation of benzaldehyde to benzoic acid is energetically not favorable, which explains the high catalytic selectivity observed experimentally.

We also carried out electrochemical oxidation of toluene using a TEMPO-modified glassy carbon electrode (TEMPO-GCE) as a catalyst. By contrast, homogeneous catalysis of toluene oxidation by TEMPO does not occur, suggesting that the standard potential of TEMPO is too low

for efficient homogeneous catalysis of toluene oxidation. While the mechanism of toluene oxidation has yet to be elucidated, previous studies suggest that C(sp^3)-H bond cleavage is the rate-determining step.[37,38] Here we show that in voltage-driven catalysis this step can be facilitated by the applied potential.

EXPERIMENTAL SECTION

Chemicals and materials. TEMPO, 4-amino-TEMPO, benzyl alcohol, 1,3,5-trimethoxybenzene, and tetrabutylammonium hexafluorophosphate ($TBAPF_6$) were purchased from Sigma-Aldrich. 2,6-dimethyl pyridine was purchased from Fisher Scientific. Sodium phosphate and sodium phosphate monobasic (Sigma-Aldrich) were used to make 0.1 M phosphate buffer (pH 7.2). Toluene and acetonitrile were purchased from Merck. All aqueous solutions were prepared using water from Milli-Q Advantage A10 system (Millipore Corp.) equipped with Q-Gard T2 Pak, a Quantum TEX cartridge, and a VOC Pak with total organic carbon (TOC) ≤ 1 ppb.

Instruments and procedures. Electrochemical experiments were carried out using a CHI 760E bipotentiostat (CH Instruments) inside a Faraday cage. In a three-electrode setup, a 3 mm diameter GCE (CH Instruments) was used as a working electrode, a Pt wire was used as a counter electrode was a Pt wire, and a commercial Ag/AgCl (1 M KCl) in aqueous solutions or $Ag/AgNO_3$ in acetonitrile served as a reference electrode. Bulk electrolysis experiments were carried out at a constant potential (1.1 V vs. $Ag/AgNO_3$) with a 3-mm-diameter, 9-mm-long TEMPO-modified graphite rod working electrode, a bare graphite rod as a counter electrode, and $Ag/AgNO_3$ reference in acetonitrile containing 0.1 M $TBAPF_6$. An undivided cell was used for the electrolysis in air atmosphere. The crude solution after the electrolysis was used for the detection of products. All voltammograms were recorded with 90% Ohmic-drop compensation.

Spectroscopic techniques, including UV-Vis, FTIR, NMR were employed to detect/characterize the products formed during electrolysis. The UV-Vis spectra were recorded using an Agilent 8453 G1103A spectrophotometer. FTIR spectra were obtained with a Bruker Alpha II spectrometer, and ^{1}H-NMR spectra were obtained using a 500 kHz Bruker instrument.

Chemical modification of carbon surface. 4-amino-TEMPO was immobilized on the carbon electrode surface through an amine linkage using the reported procedure.[39] Briefly, the GCE was biased at +0.45 V vs. Ag/AgCl for 5 mins in 0.1 M phosphate buffer (pH 7). Then, the modified electrode was washed with deionized water several times to remove physisorbed molecules. Characteristic oxidation-reduction waves of surface-bound TEMPO were obtained at the modified electrode in acetonitrile containing 0.1 M $TBAPF_6$.

Computational methods. DFT calculations were performed by using the Vienna *ab initio* simulation package (VASP).[40,41] Electron exchange-correlation was represented by the functional of Perdew, Burke and Ernzerhof (PBE) of generalized gradient approximation (GGA).[42] The ion-electron interaction was described with the projector augmented wave (PAW) method.[43] The organic solvent was treated with a continuum dielectric model, as implemented in the VASPsol code.[44,45] More computational details can be found in Supporting Information.

RESULTS & DISCUSSION

Cyclic voltammograms (CVs) were recorded at a bare GCE in acetonitrile solution containing TEMPO (Fig. 2A) and at the same GCE after immobilizing TEMPO on its surface (Fig. 2B). The surface peaks of TEMPO in Fig. 2B are about 101 mV more positive than the mid-peak potential measured with TEMPO dissolved in the same electrolyte solution (Fig. 2A). This shift reflects the effect of the potential drop on the surface-bound TEMPO molecule located within the EDL. As expected for a surface-attached reversible redox mediator, the anodic and cathodic peak

potentials in Fig. 2B are essentially independent of the scan rate (v), and the background-subtracted peak current is directly proportional to v (Fig. S2). The surface coverage, Γ_{TEMPO} = 14 pmol/cm^2 was obtained from CVs by integrating the area under the oxidation peak after background subtraction. The coverage value corresponds to <10% of the full monolayer coverage. The reported value for full monolayer coverage of TEMPO is about 2 × 10^{-10} mol/cm^2.[39] The electrochemical stability of TEMPO-GCE can be seen from 10 consecutive voltammetric cycles recorded in acetonitrile containing 0.1 M $TBAPF_6$ (Fig. S3). No significant change in peak currents/potentials was observed in this experiment.

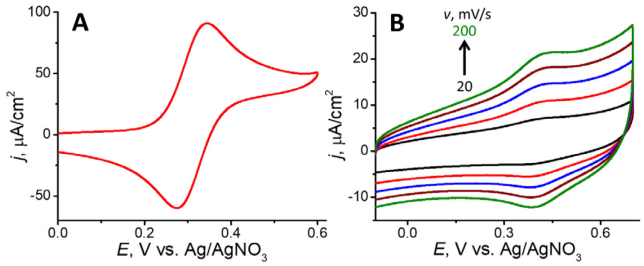

Fig. 2. CVs of (A) dissolved and (B) surface-bound TEMPO at a 3 mm GCE. Acetonitrile solution contained 0.1 M $TBAPF_6$ and either 5 mM TEMPO (A) or no TEMPO (B). v, mV/s = (A) 20; and (B) 20 (black), 50 (red), 100 (blue), 150 (brown), and 200 (green).

Voltage-driven BzOH oxidation by TEMPO. TEMPO exhibits modest activity as a homogeneous catalyst for electrochemical oxidation of BzOH in acetonitrile without added base (Fig. 3A). There are only minor differences between quasi-reversible CVs of TEMPO at a GCE obtained with no benzyl alcohol (Fig. 3A, curve 1) and with 5 mM BzOH added to the solution (Fig. 3A, curve 2). A TEMPO-GCE shows a much higher catalytic activity towards BzOH oxidation (Fig. 3B). The current onset at ~0.4 V corresponds to the TEMPO oxidation wave which is supposed to be complete at $E \approx 0.5$ V (Fig. 2B). The catalytic current continues to increase over a wide potential range (~800 mV), which cannot be attributed to direct oxidation of BzOH on the

carbon surface because the current recorded at a bare GCE (curve 2 in Fig. 3B) is much lower than that in curve 1. The current increase over a wide potential range is characteristic of voltage-driven molecular catalysis[18,19] and not observed in conventional molecular catalysis, where the anodic current should reach a plateau when the applied potential becomes sufficiently positive for complete oxidation of surface-bound mediator species.[46] A much higher catalytic activity was observed for BzOH oxidation in presence of a base with TEMPO modified electrode (Fig. 3C) in accord with the literature data.[34] The base facilitates the oxidation process by abstracting protons from the intermediates (e.g., TEMPO-H) for faster regeneration of the catalyst. The catalytic current is proportional to the concentration of BzOH (the inset in Fig. 3C).

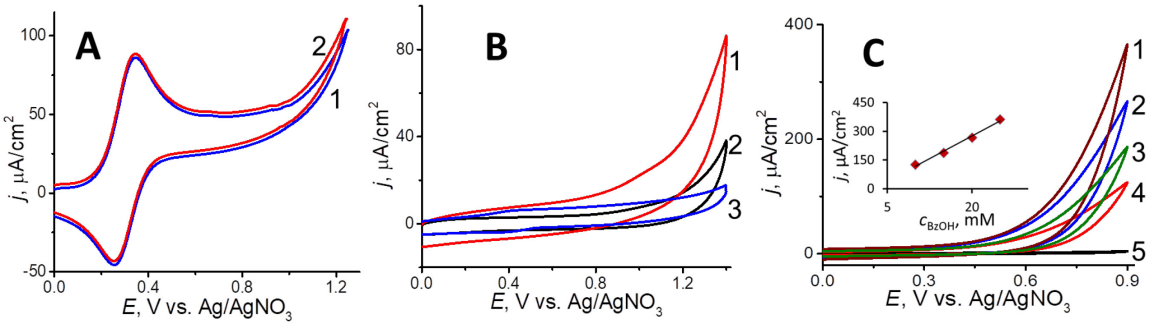

Fig. 3. Catalysis of benzyl alcohol oxidation by TEMPO in acetonitrile solutions containing 0.1 M $TBAPF_6$. (A) CVs recorded at a bare GCE in solution containing 5 mM TEMPO and either 0 (1) or 10 mM (2) of BzOH. (B) CVs of 10 mM BzOH at a TEMPO-GCE (1), bare GCE (2), and TEMPO-GCE without BzOH (3). (C) CVs of BzOH at a TEMPO-GCE in the presence of 50 mM lutidine. c_{BzOH}, mM = 25 (1), 20 (2), 15 (3), 10 (4) and 0 (5). v = 20 mV/s. The inset: concentration dependence of the current density at E = 0.9 V.

The products of BzOH oxidation were analyzed by UV-Vis spectroscopy of the crude solution after bulk electrolysis in the absence of base (Fig. 4). 2 μL of the crude solution was diluted by 3 mL of acetonitrile, containing 0.1 M $TBAPF_6$, and the resulting solution was used for UV-Vis spectroscopy to avoid oversaturation in the spectra. The UV-Vis spectra (Fig. 4A) were

obtained after 1-hour-long electrolysis at a bare (curve 1) and TEMPO-modified (curve 2) graphite rod electrode biased at a constant potential, E =1.1 V vs. $Ag/AgNO_3$. The formation of benzaldehyde at the TEMPO-modified electrode is evident from the characteristic absorption peaks at 243 nm (C=C) and 285 nm (C=O). In contrast, no benzaldehyde was detected after the BzOH electrolysis at a bare graphite electrode under the same conditions (Fig. 4A, curve 1). Only a weak absorption peak corresponding to BzOH (~260 nm) was observed. To assess the effect of the applied potential on BzOH oxidation catalysis, three UV-Vis spectra shown in Fig. 4B were recorded in solutions after bulk electrolysis at 0.9 V (curve 1), 1.1 V (curve 2), and 1.3 V vs. $Ag/AgNO_3$ (curve 3). The significant increase in benzaldehyde concentration with the applied potential is consistent with the CV response (curve 1 in Fig. 3B), pointing to the voltage-driven molecular catalysis by surface-bound TEMPO.

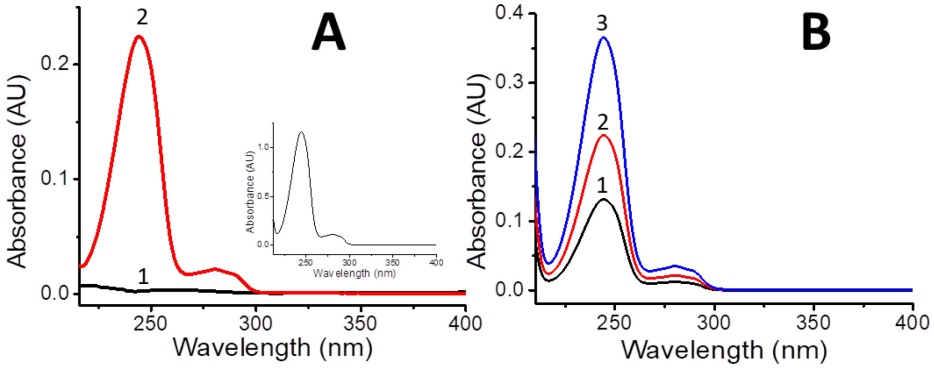

Fig. 4. Detection of benzaldehyde by UV-Vis spectroscopy after one hour bulk electrolysis of BzOH. The 2 µL volume of the crude solution containing 1 mmol BzOH and 0.1 M $TBAPF_6$ in acetonitrile was electrolyzed and then diluted by 3 mL of acetonitrile containing 0.1 M $TBAPF_6$. The working electrode was either a bare (curve 1 in A) or a TEMPO-modified (curve 2 in A and all curves in B) carbon rod. E, V vs. $Ag/AgNO_3$ = (A) 1.1; and (B) 0.9 (1), 1.1 (2), and 1.3 (3). The inset: a UV-Vis spectrum of benzaldehyde.

The amount of benzaldehyde (0.2 mmol) formed during the bulk electrolysis of 1 mmol benzyl alcohol without lutidine in acetonitrile containing 0.1 M $TBAPF_6$ was calculated from the UV-Vis calibration curve (Fig. S18A). This amount was used for the calculation of the turnover number (14 x 10^6). The Faradaic efficiency (81%) was calculated from the *i-t* curve obtained during the bulk electrolysis (Fig. S18B).

To evaluate stability/reusability of TEMPO-modified electrodes in BzOH oxidation, the same TEMPO-graphite rod was used in three constant-potential electrolysis experiments. UV-VIS spectra obtained after each one-hour-long electrolysis of BzOH at E = 1.1 V (Fig. S4) showed very similar benzaldehyde peaks. This observation suggests that the TEMPO-modified graphite electrodes are stable under electrolysis conditions and can be reused without noticeable activity loss.

We also carried out benzyl alcohol oxidation in a pH 7 aqueous buffer solution. Previous experiments showed a higher catalytic activity of TEMPO for BzOH oxidation in basic media, while homogeneous catalysis in acidic and neutral solutions was negligibly slow.[29] CVs of BzOH were recorded in 0.1 M PBS at a modified GCE (Figure 5; curves 1, 2, and 3) and a bare

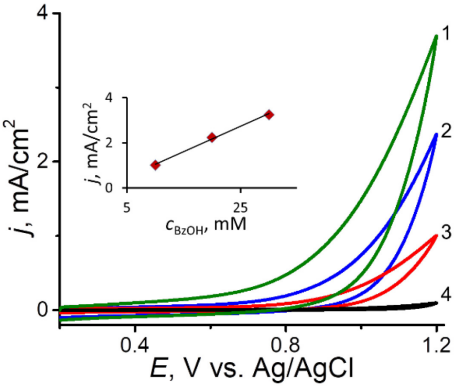

Fig. 5. CVs of BzOH at a TEMPO-GCE. c_{BzOH}, mM = 30 (1), 20 (2), and 10 (3) in 0.1 PBS of pH 7. Curve 4 is the voltammogram of 20 mM BzOH at a bare GCE. v = 20 mV/s. Inset: concentration dependence of the current density at E = 1.2 V.

GCE (curve 4). In sharp contrast to slow homogeneous catalysis, the efficient oxidation of BzOH at a TEMPO-GCE at pH 7 is due to the contribution of the electrostatic potential drop across the EDL to the driving force for this process. The voltage-driven catalysis at TEMPO-GCE in the neural aqueous buffer is faster than in acetonitrile solution without added base (*cf.* curve 2 in Fig. 3B).

Toluene oxidation at TEMPO-modified carbon electrodes. TEMPO-modified carbon electrodes also exhibit efficient voltage-driven molecular catalysis toward toluene oxidation reaction in sharp constant with immeasurably slow homogeneous catalysis by dissolved TEMPO. Indistinguishable CVs obtained in the presence (red) and absence (black) of toluene in acetonitrile solution (Fig. 6A) suggest that the standard potential of TEMPO is too low for efficient homogeneous catalysis of toluene oxidation, whereas a TEMPO-modified electrode shows voltage-driven catalytic oxidation of toluene and the catalytic current is proportional to the concentration of toluene (Fig. 6B).

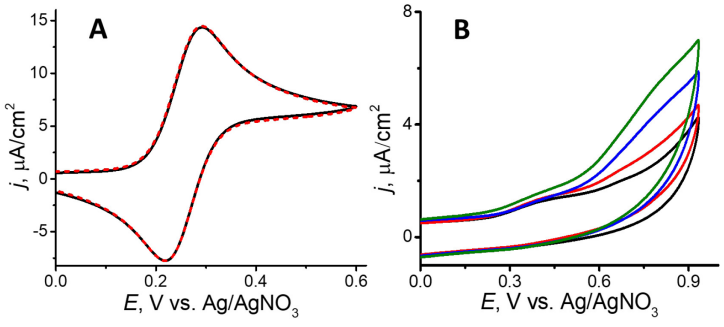

Fig. 6. CVs of oxidation of toluene in acetonitrile at the (A) bare GCE and (B) TEMPO-modified GCE. (A) $c_{toluene}$, mM = 0 (black), 20 (red); c_{TEMPO} = 0.5 mM. (B) $c_{toluene}$, mM = 0 (black), 10 (red), 20 (blue), and 30 (green). All solutions contained 0.1 M $TBAPF_6$ and 50 mM 2,6-lutidiene. v = 5 mV/s.

We used FTIR and NMR to analyze the products of BzOH and toluene oxidations. The analysis of the products in the crude solution was carried out after three hours of constant potential electrolysis. FTIR spectra were obtained before and after the electrolysis (Fig. S5 and S6), and the characteristic carbonyl stretch (~1700 cm^{-1}) was observed only after the oxidation. NMR spectra of the crude solutions were used to detect the aldehyde formed during the electrolysis of BzOH (either without lutidine, Fig. S7, or with lutidine added to the solution, Fig. S8) and toluene (Fig. S9). A strong peak observed around 10 ppm corresponds to the aldehyde functional group. The NMR yield of aldehyde was calculated using 1,3,5-trimethoxybenzene as an internal standard. The TEMPO-modified electrode selectively oxidized both BzOH and toluene to benzaldehyde. Benzoic acid was not detected in solutions after the electrolysis of benzyl alcohol, probably, due to the absence of water in the media, as reported earlier.[47,48] For the BzOH oxidation, the NMR yields were 52% (without lutidine), and 88% (with lutidine); and 42% yield was found for the toluene oxidation.

Benzaldehyde was detected in the crude solution obtained after the electrolysis of toluene at a TEMPO-modified electrode (Fig. S6 and S9), but no aldehyde was found after the electrolysis at a bare carbon electrode with TEMPO dissolved in solution. The IR spectra obtained before and after the electrolysis of toluene (S10A) and BzOH (S10B) with TEMPO dissolved in solution show no peak for carbonyl stretching. An important implication is that the applied voltage can enable the catalysis of an electro-organic reaction by a surface-bound redox mediator that would not be possible without the contribution of the electrode potential to the driving force. To check the stability of TEMPO-modified carbon electrode, CV (S11) was recorded before and after the electrolysis of BzOH. The heights of the background-subtracted peaks of TEMPO in the CVs are

essentially unchanged after an hour of electrolysis, suggesting that the grafted catalyst remains attached to the electrode surface.

The capacity of surface-bound TEMPO to oxidize both benzylic alcohol and the methyl group of toluene brings up an important question about selectivity of voltage-driven catalysis. The selective oxidation with a voltage-driven TEMPO catalyst can be attained by correctly choosing the experimental conditions. For instance, comparing the oxidations of 10 mM toluene (red curve in Fig. 6B) and 10 mM BzOH (red curve in Fig. 3C) in acetonitrile containing 50 mM 2,6-lutidiene, one can see that at E = 0.8 V, the current density for BzOH (~75 $\mu A/cm^2$) is more than 50 times that for toluene (~1 $\mu A/cm^2$ after background subtraction). An even better selectivity can be attained with no base added to the solution. The oxidation of 10 mM BzOH at GCE-TEMPO in acetonitrile without 2,6-lutidiene (red curve in Fig. 3B) produced the current density of ~30 $\mu A/cm^2$ at E = 1 V, while no measurable current was observed for the oxidation of toluene under the same conditions.

DFT simulations of voltage-driven BzOH and toluene oxidations by TEMPO. Recent DFT calculations revealed that the potential drop between surface-bound redox species and dissolved reactant molecules in aqueous solutions can contribute to the driving force for a catalytic outer-sphere or inner-sphere ET reaction.[18,19] Here, we calculated the plane-averaged electrostatic potentials for TEMPO-GCE in acetonitrile at different values of the electrode potential (Fig. S16 shows the xy-averaged potential as a function of distance along z-axis at the electrode potential of 0.29 V). As shown in Fig. 7B, similar to the aqueous solution, the electrostatic potential drops on both sides of the attached TEMPO. However, the magnitude of the potential drop between surface-bound TEMPO and solution is larger because the dielectric constant of acetonitrile is smaller than that of water. Specifically, about 1/5 of the applied potential drops between surface-bound

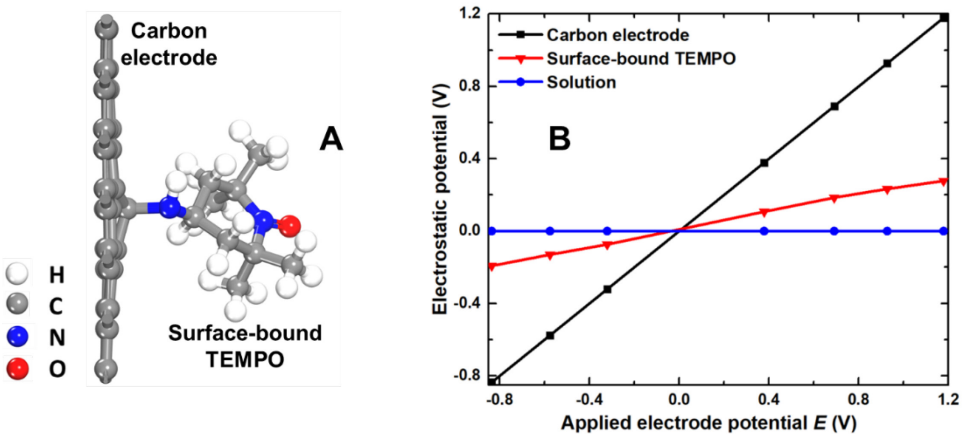

Fig. 7. TEMPO-modified carbon electrode in acetonitrile. (A) The optimized geometry of surface-bound TEMPO. (B) Plane-averaged electrostatic potentials of the carbon electrode, surface-bound TEMPO in acetonitrile, and solution as a function of the applied electrode potential, E (vs. E_{PZC}).

TEMPO and solution. This agrees well with the experimental observation that the mid-peak potential of surface-bound TEMPO is 101 mV more positive than that of TEMPO dissolved in acetonitrile (Fig. 2). Thus, this potential drop (E_2 in Fig. 1) can provide additional driving force for electrooxidations of BzOH and toluene.

The mechanism of BzOH oxidation catalyzed by TEMPO involves the formation of an adduct between TEMPO and BzOH (Fig. 8A) followed by the rate-determining intramolecular hydrogen transfer to produce TEMPOH and benzaldehyde (Fig. 8B).[36] We calculated the activation energy of the rate-determining step for TEMPO dissolved in acetonitrile and surface-bound TEMPO at different electrode potentials (Fig. 8C and Fig. S12, more details on activation energy calculations and transition state searches can be found in Computational Details and Table S1). The activation energy for TEMPO dissolved in acetonitrile is moderate (0.21 eV), which explains the experimentally observed modest homogeneous catalysis of BzOH oxidation (Fig. 3A), whereas for TEMPO-GCE, the activation energy decreases as the applied potential becomes more positive. This finding is consistent with the faster reaction rates at higher anodic potentials and

can be explained by the changes in the orbital interactions between TEMPO and BzOH substrate (Fig. S13).

We further investigated benzaldehyde oxidation to benzoic acid. The oxidation of aldehyde is deemed to involve its hydration and dissociation of the hydroxy group, followed by analogous adduct formation and intramolecular hydrogen transfer.[49] The high activation energy, 1.63 eV, found for the first step (i.e., the hydration) suggests that the oxidation of BzOH to benzoic acid is not favorable. This result agrees with the experimental finding of high catalytic selectivity of BzOH oxidation to benzaldehyde.

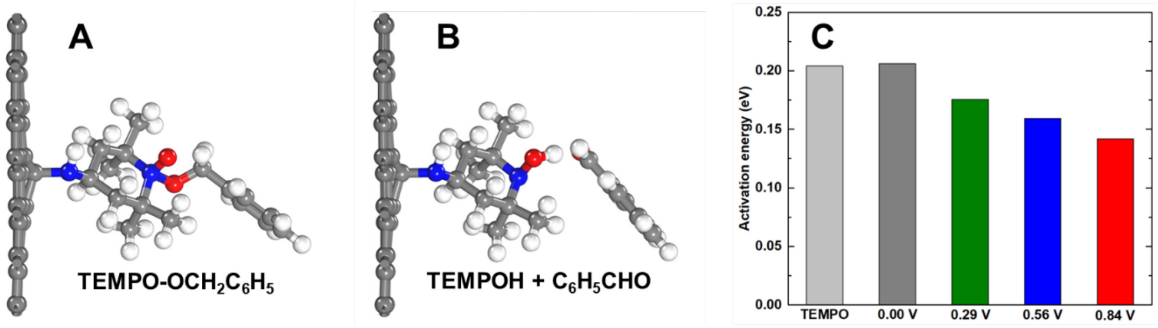

Fig. 8. BzOH oxidation catalysis by surface-bound TEMPO in acetonitrile. (A) The optimized geometry of the TEMPO-$OCH_2C_6H_5$ intermediate. (B) Formation of benzaldehyde and TEMPOH after the intramolecular hydrogen transfer. (C) Activation energy of the rate-determining step at different electrode potentials. The activation energy for TEMPO dissolved in acetonitrile is shown for comparison.

Direct electrochemical oxidation of toluene is generally initiated by outer-sphere ET followed by the rapid proton transfer and the second ET to generate a benzylic cation, which requires a high electrode potential. Recent experimental studies showed that mediated oxidation of toluene involves hydrogen atom transfer from the benzylic C–H bond to form a benzylic radical intermediate.[50] We calculated the activation energy of the hydrogen transfer step for toluene oxidation catalyzed by surface-bound TEMPO. The optimized geometries of the initial and final

states are shown in Fig. 9. The increase in applied potential from 0 V to 0.84 V results in about 50% lower activation energy, which in turn leads to much higher catalytic currents at more positive electrode potentials. By contrast, the activation energy for TEMPO dissolved in acetonitrile is as high as 0.90 eV (Fig. S14), and no measurable homogeneous catalysis of toluene oxidation by TEMPO was observed (Fig. 6A).

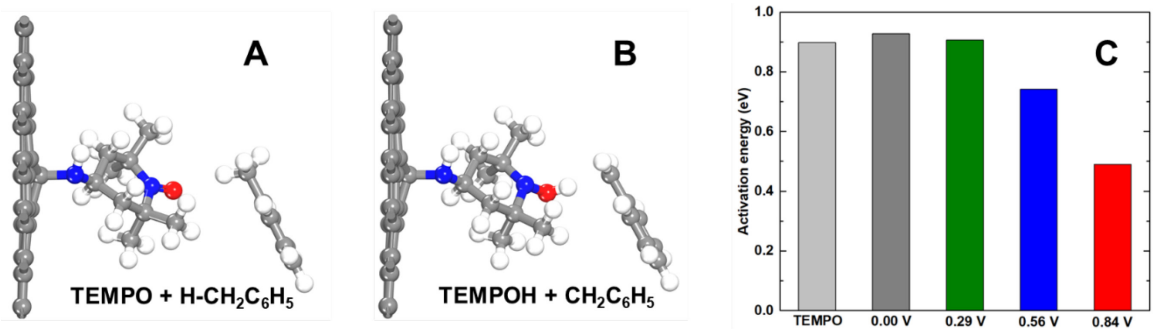

Fig. 9. Toluene oxidation electrocatalysis by surface-bound TEMPO in acetonitrile. The optimized geometries of the initial (A) and final (B) states for the sp^3 C-H bond cleavage. (C) Activation energy of this step at different electrode potentials. The activation energy for TEMPO dissolved in acetonitrile is shown for comparison.

Further electronic structure analysis reveals a correlation between the activation energy and Bader charge on oxygen of TEMPO (Fig. S15). This suggests that the sp^3 C-H bond cleavage of toluene is driven by the stronger oxidizing power of TEMPO at a higher electrode potential rather than the electrostatic potential gradient, since hydrogen atom is not charged. To better understand the electron density effect, we plotted the plane-averaged electron density difference between 0 V and 0.29 V (vs. E_{PZC}). As shown in Figure S17, there is an electron density gradient from the carbon substrate to the immobilized TEMPO, similar to the double layer potential gradient. This is analogous to adding an electron withdrawing group to the molecular catalyst. Taken together, we believe the electron density gradient could be more important for reactions

with H-abstraction as the rate-limiting steps (e.g., the toluene oxidation discussed in this work), while the electrostatic potential gradient is more important to reactions involving transfer of charged species across the double layer. Our calculations show that the rate of the molecular catalysis of toluene oxidation by surface-bound TEMPO is increased by the applied bias through reducing the activation energy for the rate-determining hydrogen-transfer step.

CONCLUSIONS

We demonstrate the first application of the recently developed concept of voltage-driven molecular catalysis to electrosynthesis. The electrode potential contribution to the catalytic driving force enabled efficient oxidation of toluene in acetonitrile and benzyl alcohol in neutral aqueous solution by purely organic TEMPO radical covalently attached to the carbon electrode surface. Our DFT calculations suggest that the applied bias causes the decrease in activation energy of the rate-determining step for TEMPO catalyzed oxidations of BzOH and toluene, thus contributing to the enhanced catalysis. Without electrostatic contribution, the homogenous catalysis of both oxidation processes by TEMPO is slow. The analysis of the products confirmed the formation of benzaldehyde and showed no detectable concentration of benzoic acid, pointing to selectivity of both catalytic processes. A very low load and ease of recycling further distinguish this approach from homogeneous molecular catalysis. These results suggest a new route for designing next-generation hybrid molecular/electrocatalysts for organic synthesis.

Supporting Information. Supplementary electrochemical data, CVs, UV-Vis, FTIR and ^{1}H NMR spectra, projected density of states for the TEMPO-$OCH_2C_6H_5$ adduct, energy profiles for the hydrogen transfer step, and computational details. This material is available free of charge via the Internet at http://pubs.acs.org.

ACKNOWLEDGMENTS

The support of this work by the National Science Foundation grant CHE-2247262 is gratefully acknowledged. This research used resources of the National Energy Research Scientific Computing Center, a DOE Office of Science User Facility supported by the Office of Science of the U.S. Department of Energy under Contract No. DE-AC02-05CH11231 using NERSC award BES-ERCAP0023976. DFT simulations were conducted as part of a user project at the Center for Nanophase Materials Sciences (CNMS), which is a US Department of Energy, Office of Science User Facility at Oak Ridge National Laboratory. The authors thank Ashif I. Bhuiyan for helping in NMR experiments.

COMPETING INTERESTS STATEMENT

The authors declare that they have no conflict of interest.

REFERENCES

1. Siu, J. C.; Fu, N.; Lin, S. Catalyzing Electrosynthesis: A Homogeneous Electrocatalytic Approach to Reaction Discovery. *Acc. Chem. Res.* **2020**, *53*, 547–560.
2. Franckle, R.; Little, R. D. Redox catalysis in organic electrosynthesis: basic principles and recent developments. *Chem. Soc. Rev.* **2014**, *43*, 2492–2521.
3. Gandeepan, P.; Finger, L. H.; Meyer, T. H.; Ackermann, L. 3d Metallaelectrocatalysis for Resource Economical Syntheses. *Chem. Soc. Rev.* **2020**, *49*, 4254-4272.
4. Novaes, L. F. T.; Liu, J.; Shen, Y.; Lu, L.; Meinhardt, J. M.; Lin, S. Electrocatalysis as an enabling technology for organic synthesis. *Chem. Soc. Rev.* **2021**, *50*, 7941-8002.
5. Malapit, C. A.; Prater, M. B.; Cabrera-Pardo, J. R.; Li, M.; Pham, T. D.; McFadden, T. P.; Blank, S.; Minteer, S. D. Advances on the Merger of Electrochemistry and Transition Metal Catalysis for Organic Synthesis. *Chem. Rev.* **2022**, *122*, 3180−3218.
6. Pollok, D.; Waldvogel, S. R. Electro-organic synthesis – a 21st century technique. *Chem. Sci.* **2020**, *11*, 12386-12400.
7. Li, J.; Triana, C. A.; Wan, W.; Adiyeri Saseendran, D. P.; Zhao, Y.; Balaghi, S. E.; Heidari, S.; Patzke, G. R. Molecular and heterogeneous water oxidation catalysts: recent progress and joint perspectives. *Chem. Soc. Rev.* **2021**, *50*, 2444-2485.
8. Yang, Y.; Peltier, C. R.; Zeng, R.; Schimmenti, R.; Li, Q.; Huang, X.; Yan, Z.; Potsi, G.; Selhorst, R.; Lu, X.; Xu, W.; Tader, M.; Soudackov, A. V.; Zhang, H.; Krumov, M.; Murray,

E.; Xu, P.; Hitt, J.; Xu, L.; Ko, H.-Y.; Ernst, B. G.; Bundschu, C.; Luo, A.; Markovich, D.; Hu, M.; He, C.; Wang, H.; Fang, J.; DiStasio, R. A., Jr.; Kourkoutis, L. F.; Singer, A.; Noonan, K. J. T.; Xiao, L.; Zhuang, L.; Pivovar, B. S.; Zelenay, P.; Herrero, E.; Feliu, J. M.; Suntivich, J.; Giannelis, E. P.; Hammes-Schiffer, S.; Arias, T.; Mavrikakis, M.; Mallouk, T. E.; Brock, J. D.; Muller, D. A.; DiSalvo, F. J.; Coates, G. W.; Abruña, H. D. Electrocatalysis in Alkaline Media and Alkaline Membrane-Based Energy Technologies. *Chem. Rev.* **2022**, *122*, 6117−6321.

9. Wu, L.; Nayak, A.; Shao, J.; Meyer, T. J. Crossing the bridge from molecular catalysis to a heterogenous electrode in electrocatalytic water oxidation. *Proc. Natl. Acad. Sci. USA* **2019**, *116*, 11153-11158.
10. Nong, H. N.; Falling, L. J.; Bergmann, A.; Klingenhof, M.; Tran, H. P.; Spöri, C.; Mom, R.; Timoshenko, J.; Zichittella, G.; Knop-Gericke, A.; Piccinin, S.; Pérez-Ramírez, J.; Cuenya, B. R.; Schlögl, R.; Strasser, P.; Teschner, D.; Jones, T. E. Key role of chemistry versus bias in electrocatalytic oxygen evolution. *Nature* **2020**, *587*, 408–413.
11. Boettcher, S. W.; Surendranath, Y. Heterogeneous electrocatalysis goes chemical. *Nat. Catal.* **2021**, *4*, 4–5.
12. Bates, J. S.; Biswas, S.; Suh, S.-E.; Johnson, M. R.; Mondal, B.; Root, T. W.; Stahl, S. S. Chemical and electrochemical O_2 reduction on earth-abundant M-N-C catalysts and implications for mediated electrolysis. *J. Am. Chem. Soc.* **2022**, *144*, 922-927.
13. Yuan, Y.; Lei, A. Is electrosynthesis always green and advantageous compared to traditional methods? *Nat. Commun*. **2020**, *11*, 802.
14. Marchetti, P.; Jimenez Solomon, M. F.; Szekely, G.; Livingston, A. G. Molecular separation with organic solvent nanofiltration: a critical review. *Chem. Rev.* **2014**, *114*, 10735–10806.
15. Oh, S.; Gallagher, J. R.; Miller, J. T.; Surendranath, Y. Graphite-conjugated rhenium catalysts for carbon dioxide reduction. *J. Am. Chem. Soc.* **2016**, *138*, 1820−1823.
16. Jackson, M. N.; Surendranath, Y. Molecular control of heterogeneous electrocatalysis through graphite conjugation. *Acc. Chem. Res.* **2019**, *52*, 3432–3441.
17. Jackson, M. N.; Oh, S.; Kaminsky, C. J.; Chu, S. B.; Zhang, G.; Miller, J. T.; Surendranath, Y. Strong Electronic Coupling of Molecular Sites to Graphitic Electrodes via Pyrazine Conjugation. *J. Am. Chem. Soc.* **2018**, *140*, 1004–1010.
18. Barman, K.; Wang, X.; Jia, R.; Askarova, G.; Hu, G.; Mirkin, M. V. Voltage-driven molecular catalysis of electrochemical reactions. *J. Am. Chem. Soc.* **2021**, *143*, 17344−17347.
19. Barman, K.; Askarova, G.; Jia, R.; Hu, G.; Mirkin, M. V. Efficient Voltage-Driven Oxidation of Water and Alcohols by Organic Molecular Catalyst Directly Attached to a Carbon Electrode. *J. Am. Chem. Soc.* **2023***, 145*, 5786−5794.
20. Yan, M.; Kawamata, Y.; Baran, P. S. Synthetic organic electrochemical methods since 2000: on the verge of a renaissance. *Chem. Rev.* **2017**, *117*, 13230–13319.
21. Nutting, J. E.; Rafiee, M.; Stahl, S. S. Tetramethylpiperidine N-oxyl (TEMPO), phthalimide N-oxyl (PINO), and related N-oxyl species: electrochemical properties and their use in electrocatalytic reactions. *Chem. Rev.* **2018**, *118*, 4834−4885.

22. de Nooy, A. E. J.; Besemer, A. C.; van Bekkum, H. On the Use of Stable Organic Nitroxyl Radicals for the Oxidation of Primary and Secondary Alcohols. *Synthesis* **1996**, *1996*, 1153−1176.
23. Sheldon, R. A.; Arends, I. W. C. E. Organocatalytic Oxidations Mediated by Nitroxyl Radicals. *Adv. Synth. Catal*. **2004**, *346*, 1051− 1071.
24. Bobbitt, J. M.; Brückner, C.; Merbouh, N. Oxoammonium- and Nitroxide-Catalyzed Oxidations of Alcohols. *Org. React.* **2009**, *74*, 103– 424.
25. Wertz, S.; Studer, A. Nitroxide-Catalyzed Transition-Metal-Free Aerobic Oxidation Processes. *Green Chem*. **2013**, *15*, 3116−3134.
26. Vogler, T.; Studer, A. Applications of TEMPO in Synthesis. *Synthesis* **2008**, *2008*, 1979−1993.
27. Nutting, J. E.; Rafiee, M.; Stahl, S. S. Tetramethylpiperidine N- Oxyl (TEMPO), phthalimide N-oxyl (PINO), and related N-oxyl species: electrochemical properties and their use in electrocatalytic reactions. *Chem. Rev.* **2018**, *118*, 4834–4885.
28. Hill-Cousins, J. T.; Kuleshova, J.; Green, R. A.; Birkin, P. R.; Pletcher, D.; Underwood, T. J.; Leach, S. G.; Brown, R. C. D. TEMPO-Mediated Electrooxidation of Primary and Secondary Alcohols in a Microfluidic Electrolytic Cell. *ChemSusChem* **2012**, *5*, 326−331.
29. Rafiee, M.; Miles, K. C.; Stahl, S. S. Electrocatalytic Alcohol Oxidation with TEMPO and Bicyclic Nitroxyl Derivatives: Driving Force Trumps Steric Effects. *J. Am. Chem. Soc*. **2015**, *137*, 14751− 14757.
30. Yan, M.; Kawamata, Y.; Baran, P. S. Synthetic Organic Electrochemical Methods Since 2000: On the Verge of a Renaissance. *Chem. Rev.* **2017**, *117*, 13230–13319.
31. Hickey, D. P.; Milton, R. D.; Chen, D.; Sigman, M. S.; Minteer, S. D. TEMPO-Modified Linear Poly(Ethylenimine) for Immobilization-Enhanced Electrocatalytic Oxidation of Alcohols. *ACS Catal.* **2015**, *5*, 5519−5524.
32. Das, A.; Stahl, S. S. Noncovalent Immobilization of Molecular Electrocatalysts for Chemical Synthesis: Efficient Electrochemical Alcohol Oxidation with a Pyrene-TEMPO Conjugate. *Angew. Chem. Int. Ed.* **2017**, *56*, 8892−8897.
33. Rafiee, M.; Karimi, B.; Alizadeh, S. Mechanistic Study of the Electrocatalytic Oxidation of Alcohols by TEMPO and NHPI. *ChemElectroChem* **2014**, *1*, 455−462.
34. Niu, P. F.; Cai, Y. C.; Guo, M.; Shen, Z. L.; Li, M. C. Preparation and Electrochemical Performance of TEMPO-modified Polyterthiophene Electrode Obtained by Electropolymerization. *Electrochem. Commun*. **2020**, *110*, 106623–106628.
35. Hahn, Y.; Song, S. K. Electrochemical Behavior of a TEMPO-Modified Electrode and Its Electrocatalytic Oxidation of Benzyl Alcohol. *Anal. Sci.* **1997**, *13*, 329-332.
36. Semmelhack, M. F.; Schmid, C. R.; Cortés, D. A. Mechanism of the oxidation of alcohols by 2,2,6,6-tetramethylpiperdine nitrosonium cation. *Tetrahedron Lett.* **1986**, *27*, 1119-1122.
37. Ma, Y.; Yao, X.; Zhang, L.; Ni, P.; Cheng, R.; Ye, J. Direct Arylation of α-Amino C(sp3)-H Bonds by Convergent Paired Electrolysis. *Angew. Chem. Int. Ed.* **2019**, *58*, 16548-16552.

38. Li, C.; Zeng, C. C.; Hu, L. M.; Yang, F. L.; Yoo, S. J.; Little, R. D. Electrochemically induced C–H functionalization using bromide ion/2,2,6,6-tetramethylpiperidinyl-N-oxyl dual redox catalysts in a two-phase electrolytic system. *Electrochim. Acta* **2013**, *114*, 560-566.
39. Geneste, F.; Moinet, C. Electrochemically linking TEMPO to carbon via amine bridges. *New J. Chem.* **2005**, *29*, 269−271.
40. Kresse, G.; Furthmüller, J. Efficient iterative schemes for Ab-Initio total-energy calculations using a plane-wave basis set. *Phys. Rev. B.* **1996**, *54*, 11169-11186.
41. Kresse, G.; Furthmüller, J. Efficiency of Ab-Initio total energy calculations for metals and semiconductors using a plane-wave basis set. *Comput. Mater. Sci.* **1996**, *6*, 15-50.
42. Perdew, J. P.; Burke, K.; Ernzerhof, M. Generalized gradient approximation made simple. *Phys. Rev. Lett.* **1996**, *77*, 3865.
43. Blöchl, P. E. Projector Augmented-Wave Method. *Phys. Rev. B.* **1994**, *50*, 17953-17979.
44. Mathew, K.; Sundararaman, R.; Letchworth-Weaver, K.; Arias, T.; Hennig, R. G. Implicit solvation model for density-functional study of nanocrystal surfaces and reaction pathways. *J. Chem. Phys.* **2014**, *140*, 084106.
45. Mathew, K.; Kolluru, V. C.; Mula, S.; Steinmann, S. N.; Hennig, R. G. Implicit self-consistent electrolyte model in Plane-Wave Density-Functional Theory. *J. Chem. Phys.* **2019**, *151*, 234101.
46. Savéant, J.-M. Molecular Catalysis of Electrochemical Reactions. Mechanistic Aspects. *Chem. Rev.* **2008**, *108*, 2348–2378.
47. Badalyan, A.; Stahl, S. S. Cooperative Electrocatalytic Alcohol Oxidation with Electron-Proton-Transfer Mediators. *Nature* **2016**, *535*, 406−410.
48. Cook, A. W.; Waldie, K. M. Molecular Electrocatalysts for Alcohol Oxidation: Insights and Challenges for Catalyst Design. *ACS Appl. Energy Mater*. **2020**, *3*, 38−46.
49. Isogai, A.; Hänninen, T.; Fujisawa, S.; Saito, T. Review: Catalytic oxidation of cellulose with nitroxyl radicals under aqueous conditions. *Prog. Polym. Sci.* **2018**, *86*, 122-148.
50. Wang, F.; Stahl, S. S. Electrochemical Oxidation of Organic Molecules at Lower Overpotential: Accessing Broader Functional Group Compatibility with Electron−Proton Transfer Mediators. *Acc. Chem. Res*. **2020**, *53*, 561-574.

For TOC only

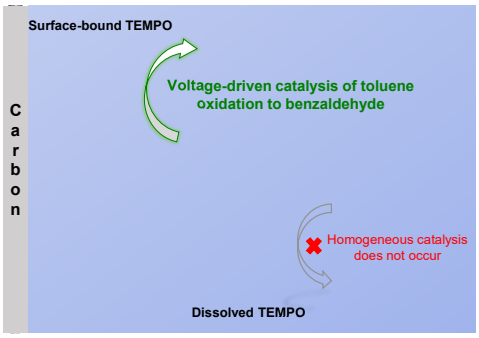
Surface-bound TEMPO
Voltage-driven catalysis of toluene oxidation to benzaldehyde
Carbon
Homogeneous catalysis does not occur
Dissolved TEMPO